Computer Science, Engineering and Technology

Vol: 1(1), March 2025

REST Publisher; ISSN: 2583-9179 (Online)

Website: https://restpublisher.com/journals/cset/

DOI: https://doi.org/10.46632/cset/1/1/9

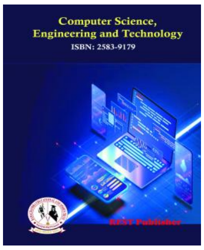

Enhanced Image Segmentation in Medical Imaging Using Mini-Net

***S. Ponlatha, M. Sweetline Sonia, M. Iswarya, R. Kanagaraj**

Mahendra Engineering College, Namakkal, Tamil Nadu, India.

*Corresponding Author Email: ponlathas@mahendra.info

Abstract. Computer-aided diagnosis and analysis of medical imaging depend on the precise segmentation of anatomical structures and anomalies. High segmentation accuracy is attained by Deep Learning (DL) algorithms; nevertheless, real-time applications are hindered by their computing needs. Furthermore, a lot of advanced segmentation techniques might not be the best for medical imaging even while they work well for segmenting objects in general. In order to improve the segmentation of medical images, this study presents Mini net, a lightweight segmentation network. Mini-Net can analyse data in real time because it efficiently records both high- and low-frequency information with less than 38,000 parameters. MoNuSeg, ISIC-2016, ISIC-2018, and DRIVE are among the benchmark datasets used to assess Mini-Net. The results show its durability and strength. Mini-Net achieves competitive accuracy compared to existing state-of-the-art methods while maintaining efficiency.

Keywords: Segmentation, Medical Imaging, Deep learning, Mini-Net, Convolutional Neural Networks.

1. INTRODUCTION

Accurately defining anatomical features or anomalies in medical images is crucial for both illness evaluation and treatment planning. Computer-assisted approaches can be more effective than manual or semiautomatic approaches, which were laborious, subjective, and vulnerable to interobserver variability. Medical picture segmentation has been transformed by DL developments, which use sizable, annotated datasets and carefully constructed neural networks to acquire intricate representations of images and accurately infer pixel-level labels. A state-of-the-art combination of computer vision and medical imaging, medical image segmentation aims to derive valuable information from complex medical images. As imaging technologies like Computed Tomography (CT), PET, and Magnetic Resonance Imaging (MRI) proliferate, it is becoming increasingly crucial to precisely identify and analyse any diseased areas or anatomical features in these pictures. This accuracy is now crucial for medical research, therapy planning, and clinical diagnosis.

For an accurate diagnosis and the best possible treatment planning, medical pictures must accurately segment anatomical structures and anomalies [1,2,3]. Even for human professionals, however, this work presents considerable difficulties because of things like unclear structural boundaries, a variety of textures, an uneven distribution of intensity, intrinsic uncertainty in segmented sections, contrast fluctuations, and a lack of annotated datasets. Numerous research initiatives have been launched in an attempt to overcome these obstacles due to the pressing need for automated segmentation algorithms in medical imaging. For instance, three multiscale kernels were used to capture big, medium, and thin vessels in a fully convolutional multiscale residual network that was proposed for retinal vascular segmentation [4]. A block matching technique and multiscale triple stick filtration method were used to segment large and thin retinal arteries [5]. To automatically identify small vessels in fundus pictures with noise, an enhanced ensemble block matching method was also suggested [6], [7]. The two main categories of segmentation methods now in use are supervised and unsupervised. Supervised methods use pairs of annotated training images to learn, while unsupervised methods use minimal characteristics and ad hoc rules without marking, which restricts their generalisability.

Digital image processing is a broad field of research that encompasses, among other things, machine vision, medical imaging, astronomy, microscopy, and geology. The process of conducting research in science and medicine involves multiple steps. When medical imaging makes it possible to automatically divide medical images and create computer-aided designs, it is an essential step. They specifically aid in improving the accuracy and scheduling of surgical treatments via the utilisation of interactions between humans and machines. In order to provide practical diagnostic tools for the medical industry, this approach consists of two components: creating imaging devices and putting a treatment plan into action. Medical tools of all kinds were used to make segment images of the human anatomy. Two of the most popular non-invasive imaging methods for taking pictures of human organs are CT and MRI.

The use of medical imaging technologies has recently moved from lab settings to patient bedsides. In order to improve patient care, this method—known as point-of-care imaging—involves conducting assessment and evaluation right next to the patient. This change anticipates more lightweight and real-time medical AI models. Point-Of-Care Ultrasound (POCUS) task switching has used in infectious conditions, obstetrics, gynaecology, medical emergencies, and cardiovascular, gastrointestinal, and lung diseases. It has an opportunity to increase medical imaging ability at primary care providers in areas with limited resources and produce significant health outcomes [8]. Point-of-care AI systems must take into account factors like instantaneous efficiency, deployability, and minimal structure. A real-time AI system and point-of-care system were created [9] to assist clinicians in diagnosing a variety of skin conditions. In such cases, segmentation that is both lightweight and fast is essential because it guarantees that the AI system can precisely and rapidly define regions of interest, enabling effective operation on devices with limited resources and delivering accurate, rapid outcomes.

Researchers have been investigating the use of lightweight techniques within neural networks in order to improve extracting features efficiency. These strategies include weight quantisation, low-rank approximation, and network pruning. Depth-wise differentiated convolutions are used in popular minimalist techniques like the MobileNet series to minimise processing and variables. To improve and balance the interactions between channels, Shufflenet and Shufflenet V2 introduce channel split and channel shuffle. In order to reduce FLOPs more, Ghostnet and CEModule use group convolutions in conjunction with depth-wise separated convolutions and a number of basic linear operations to substitute some convolutional operations. Two branches are used by BiseNet and BiseNet V2 to gather spatial and semantic data; the latter improves the framework and adds new training techniques. Due to their exceptional precision and ability to combine the advantages of Mobile Net and Transformer, lightweight Transformer techniques like Mobile-Former, ToPFormer, and MobileViT have also drawn a lot of interest. For parameter reduction, UNeXt uses mobile tokenisation MLPs (multilayer perceptrons) in place of convolutional layers.

2. LITERATURE REVIEW

Even though these models are quite effective, solutions that are specific to devices with limited resources are still required. Khan et al., have developed a macrolevel neural network system for medical picture segmentation by analysing image difficulty in order to address this difficulty. To limit the model's size and capacity, they employ a version of U-Net that has fewer filters and shallower encoder blocks [10]. Iqbal et al., have developed a small-scale neural network that reduces computational redundancy by removing feature overlap, for the purpose of segmenting retinal arteries [11]. Tariq et al., have enhanced segmentation performance by employing numerous kernels of varying sizes to optimise the field of reception [12]. Arsalan et al., have created a neural network with three million parameters for polyp classification using a multi-scale transmitted approach [13]. Razzak et al., have offered an attribute of the improvement segmentation network that eliminates the necessity for pre-training picture augmentation, hence lowering the computational cost involved [14].

Lang et al., have suggested a novel method. This approach processes features and performs fusion restoration in the decoder by using self-attention techniques, in order to preserve spatial features while collecting global contextual data [15]. Liu et al., have suggested the use of a Detailed Enhancement and Denoising block (DED) to improve the segmentation accuracy of tiny pathologic lesions [16]. Valanarasu et al., have presented UNeXt, a framework tailored for image partitioning that combines convolutional structures with MLP-based mechanisms. The architecture includes a preliminary convolutional phase, succeeded by an embedded MLP module, where tokenized MLP components reshape convolution-derived representations. This approach decreases the number of parameters and computational burden while boosting segmentation efficiency by redistributing input channels to grasp localized relationships [17].

Ruan et al., have presented EGE-UNet, which combines Group multi-axis Hadamard Product Attention (GHPA) and Group Aggregation Bridge (GAB) components to efficiently extract various pathologic details and combine multifaceted options, resulting in a much smaller network size [18]. Liu et al., have presented Rolling-UNet, which combines CNN and MLP to efficiently capture both local characteristics and long-distance dependencies, to enhance medical picture segmentation [19]. Li et al., have implemented U-KAN, an improved U-Net variant that integrates Kolmogorov-Arnold networks (KANs), in order to boost precision and accessibility in segmenting medical images and diffusion models [20,21]. This variant accomplished greater efficiency at a lower computational cost than conventional U-Net methods.

Tan et al., have suggested a straightforward yet effective composite scale technique that builds upon current baseline convolutional neural network models without compromising model validity, after a thorough analysis of the effects of network depth and width [22]. For the purpose of segmenting lesions in ultrasound images, Li et al., have presented a simplified version of U-Net. Applications with limited resources can benefit greatly from this model's ability to strike a compromise between accuracy and processing economy [23]. In order to preserve spatial features while collecting global context-related data, Lang et al., have suggested a novel method. This approach processes features and performs fusion restoration in the decoder by using self-attention techniques [24]. Liu et al., have stated the use of a detailed enhancing and denoising block (DED) to improve the classification accuracy of tiny pathologic lesions [25].

3. RESEARCH METHODOLOGY

The research methodology focuses on developing and accessing Mini-Net, a compact DL model for medical image segmentation. The model is designed with an optimized architecture to enhance segmentation accuracy while minimizing computational complexity. Training and validation are performed using benchmark datasets such as DRIVE, ISIC-2016, ISIC-2018, and MoNuSeg. Preprocessing techniques standardize input images to improve feature extraction. Mini-Net's performance is evaluated using metrics like Dice coefficient, Intersection over Union (IoU), sensitivity, and specificity. A comparative analysis is conducted against state-of-the-art methods to assess segmentation accuracy and efficiency. The study ensures robustness by testing across diverse medical imaging modalities. The lightweight design facilitates real-time processing without compromising performance. Model training utilizes optimized hyperparameters to achieve balanced learning. Data augmentation techniques enhance generalization and prevent overfitting. Statistical analysis validates the significance of Mini-Net's improvements. The results demonstrate its potential for efficient and accurate medical image segmentation.

DL Methods for Enhanced Image Segmentation in Medical Imaging: Enhanced image segmentation in medical imaging has been significantly improved with the integration of advanced DL methods. Convolutional Neural Networks (CNNs) serve as the foundation for many segmentation models, enabling efficient feature extraction and spatial analysis. Fully Convolutional Networks (FCNs) extend CNNs by replacing fully connected layers with convolutional layers, facilitating pixel-wise predictions. U-Net, a widely adopted architecture, enhances segmentation accuracy with its encoder-decoder structure and skip connections, making it effective for biomedical image segmentation. Variants such as Attention U-Net incorporate attention mechanisms to focus on relevant regions, improving segmentation precision. Transformer-based models, including Vision Transformers (ViTs) and Swin Transformers, leverage self-attention mechanisms to capture long-range dependencies in medical images. Additionally, Generative Adversarial Networks (GANs) enhance segmentation by generating realistic synthetic images for data augmentation and refining predictions. Deep reinforcement learning has also been explored to optimize segmentation strategies dynamically. Hybrid approaches, combining CNNs with transformers or incorporating multi-scale feature extraction, further enhance segmentation performance. These advancements contribute to improved diagnostic accuracy and automation in medical imaging applications.

4. MINI-NET ARCHITECTURE

Mini-Net is a lightweight DL architecture designed for efficient medical image segmentation, balancing accuracy and computational efficiency. It follows an encoder-decoder structure, incorporating depth wise separable convolutions to reduce the number of parameters while maintaining feature extraction capabilities. The encoder extracts hierarchical features through stacked convolutional layers with batch normalization and ReLU activation, while the bottleneck layer captures essential spatial and contextual information in a compact representation. The decoder reconstructs the segmented output using up sampling layers and transposed convolutions, complemented by skip connections to retain spatial details. The final segmentation mask is generated using a SoftMax activation function for multi-class segmentation or a sigmoid activation for binary tasks. This design ensures Mini-Net achieves high segmentation accuracy while enabling real-time processing in medical imaging applications.

Input Representation: Let the input medical image be represented as:

$$I \in \mathbb{R}^{H\times \mathrm{W}\times \mathrm{C}}$$

where:

- H is the height of the image.
- W is the width of the image.
- C is the number of channels (grayscale: $C = 1$, RGB: $C = 3$).

Before feeding into the network, the input image undergoes preprocessing steps such as resizing, normalization, and contrast enhancement. These preprocessing steps help improve feature extraction by ensuring consistency across datasets.

Convolutional Encoding: The encoder consists of convolutional layers designed to extract spatial and contextual features from the input image. The general form of a convolutional layer operation is:

$$F_l = \sigma(W_l * F_{l-1} + b_l)$$

where:

- F_l represents the output feature map at layer l.
- W_l is the convolutional filter (kernel) at layer l.
- $*$ denotes the convolution operation.
- b_l is the bias term added after convolution.
- σ is the activation function (ReLU).
- F_{l-1} is the input to the convolutional layer, which is either the original image (for the first layer) or the output of the previous convolutional layer.

The convolutional layer detects edges, textures, and patterns in the input image, enabling hierarchical feature extraction. Mini-Net uses depth wise separable convolutions to improve computational efficiency while maintaining expressive feature learning.

Depth wise Convolution: Unlike standard convolutions, Mini-Net uses depth wise separable convolutions, which divide the operation into two steps:

Instead of applying a single filter to all input channels, depth wise convolution applies a separate filter to each channel independently:

$$F_d^l = \sum_{k=1}^{K} W_{l,k}^{(d)} * F_{l-1,k}$$

where:

- F_d^l is the intermediate output after depthwise convolution.
- K represents the number of channels in the input feature map.
- $W_{l,k}^{(d)}$ is the depth wise filter applied to the k-th channel.
- $F_{l-1,k}$is the k -th channel of the input feature map.

This reduces the number of parameters by eliminating cross-channel interactions in this step.

Pointwise Convolution: A 1×1 convolution (pointwise convolution) is then applied to recombine the channel-wise outputs:

$$F_l = W_l^{(p)} * F_l^{(d)}$$

where:

- $W_l^{(p)}$ is the pointwise filter applied to merge information across different channels.
- $F_l^{(d)}$ is the output of the depth wise convolution.

This operation maintains spatial relationships while significantly reducing computational costs compared to traditional convolutions.

Bottleneck Feature Representation: The bottleneck layer is a crucial component of Mini-Net, compressing the feature maps while retaining critical information for segmentation. The transformation in the bottleneck layer is given by:

$$F_b = ReLU(W_b * F_{enc} + b_b)$$

where:

- F_b is the bottleneck feature representation.
- W_b and b_b are the weights and bias of the bottleneck layer.
- F_{enc} is the encoded feature map before the bottleneck.

The bottleneck ensures the network learns compact, high-level representations of the image, reducing redundant computations while preserving necessary spatial features.

Up sampling and Decoding: The decoder reconstructs the segmented image using up sampling and transposed convolutions to restore spatial resolution. The up-sampling operation is given by:

$$F_{up} = Upsample(F_b) + W_d * F_b$$

where:

- F_{up} is the feature map after up sampling.
- W_d represents the transposed convolution filter, which learns how to expand feature maps.

Additionally, skip connections are introduced to enhance segmentation accuracy. Skip connections link corresponding encoder and decoder layers, preserving fine details that may be lost during encoding:

$$F_{dec} = F_{up} + F_{enc}$$

where:

- $F_{dec}$is the final feature representation before segmentation output.

- F_{enc} is the corresponding encoder feature map.

This fusion of high-level and low-level features improves segmentation accuracy, ensuring precise boundary delineation in medical images.

The final segmentation mask is generated using an activation function applied to the output of the decoder. Two cases arise based on the type of segmentation task:

Multi-Class Segmentation (Softmax Activation): The final segmentation mask is generated using an activation function applied to the output of the decoder. Two cases arise based on the type of segmentation task:

For multi-class segmentation, each pixel is classified into one of several classes using the SoftMax function:

$$P(x) = \frac{e^{F_{out(x)}}}{\sum_j e^{F_{out(j)}}}$$

where:

- $P(x)$ is the probability of a pixel belonging to a particular class.
- $F_{out(x)}$ is the output feature at pixel x.
- The denominator ensures that the sum of probabilities for all classes at each pixel equals 1.

Binary Segmentation (Sigmoid Activation): For binary segmentation (e.g., lesion vs. non-lesion classification), the sigmoid function is used:

$$P(x) = \frac{1}{1 + e^{-F_{out(x)}}}$$

where:

- $F_{out(x)}$ is the final pixel-wise output.
- The sigmoid function maps values to a probability range of (0,1), allowing binary classification of each pixel.

The output segmentation mask provides a pixel-wise classification of anatomical structures, ensuring precise segmentation with minimal computational overhead.

Table 1. Datasets used in the study

Application	Dataset	Image Resolution	Total	Training/Test Split
Retinal Vessels	DRIVE [53]	584×565	40	Train: 20, Test: 20
Retinal Vessels	CHASEDB1 [13]	999×960	28	Train: 20, Test: 8
Skin Lesions	ISIC 2016 [16]	679×453–6,748×4,499	1,279	Train: 900, Test: 379
Skin Lesions	ISIC 2018 [8]	679×453–6,748×4,499	2,750	Train: 2,000, Test: 600
Cell Nuclei	MoNuSeg [33]	1,000×1,000 pixels	44	Train: 30, Test: 14

TABLE 2. Comparing Mini-Net's performances with several SOTA techniques on the ISIC 2018 and ISIC 2016 segmentation of skin lesions datasets.

Method	Performance (%)									
	ISIC 2018					ISIC 2016				
	$Jacc$	F_1	A_{cc}	Se	Sp	$Jacc$	F_1	A_{cc}	Se	Sp
U-Net [49]	80.09	86.64	92.52	85.22	92.09	81.38	88.24	93.31	87.28	92.88
UNet++ [64]	81.62	87.32	93.72	88.70	93.96	82.81	89.19	93.88	88.78	93.52
BCDU-Net [3]	81.10	85.10	93.70	78.50	98.20	83.43	80.95	91.78	78.11	**96.20**
CPFNet [12]	79.88	87.69	94.96	89.53	96.55	83.81	90.23	95.09	92.11	95.91
DAGAN [35]	81.13	88.07	93.24	90.72	95.88	84.42	90.85	95.82	92.28	95.68
FAT-Net [58]	82.02	89.03	95.78	91.00	96.99	85.30	91.59	96.04	92.59	96.02
AS-Net [19]	83.09	89.55	95.68	93.06	94.69	-	-	-	-	-
SLT-Net [11]	71.51	82.85	-	78.85	**99.35**	-	-	-	-	-
Ms RED [9]	83.86	90.33	96.45	91.10	-	87.03	**92.66**	96.42	-	-
ARU-GD [39]	84.55	89.16	94.23	91.42	96.81	85.12	90.83	94.38	89.86	94.65
Swin-Unet [5]	82.79	88.98	96.83	90.10	97.16	**87.60**	88.94	96.00	92.27	95.79
Mini-Net	**89.82**	**94.47**	**96.89**	**94.22**	97.78	87.17	92.45	**96.60**	**92.51**	95.34

TABLE 3. Mini-Net is contrasted with other current research on the DRIVE dataset.

Method	Se	Sp	A	F_1	Params (M)
SegNet [4]	0.7949	0.9738	0.9579	0.8182	28.40
Three-Stage FCN [63]	0.7631	0.9820	0.9538	-	20.40
Image BTS-DSN [51]	0.7800	0.9806	0.9551	0.8208	7.80
VessNet [2]	0.8022	0.9810	0.9655	-	9
DRIU [40]	0.7855	0.9799	0.9552	0.8220	7.80
Patch BTS-DSN [51]	0.7891	0.9804	0.9561	0.8249	7.8
DPN [14]	0.7934	0.9810	0.9571	0.818	3.40
MobileNet-V3 [18] (Lightweight)	0.8250	0.9771	0.9371	0.6575	2.50
ERFNet [48] (Lightweight)	-	-	0.9598	0.7652	2.06
M2U-Net [34] (Lightweight)	-	-	0.9630	0.8091	0.55
Vessel-Net [60] (Lightweight)	0.8038	0.9802	0.9578	-	1.70
MS-NFN [59] (Lightweight)	0.7844	0.9819	0.9567	-	0.40
FCN [1] (Lightweight)	0.8039	0.9804	0.9576	-	0.20
T-Net [31] (Lightweight)	0.8262	**0.9862**	0.9697	0.8269	**0.03**
ESDMR-Net (Lightweight) [30]	0.8320	0.9832	**0.9699**	0.8287	0.70
Proposed Mini-Net(Lightweight)	**0.8370**	0.9778	0.9598	**0.8412**	0.04

TABLE 4. Comparison with the MoNuSeg [26] dataset's the most recent findings

Method	J	F_1	Params (M)
U-Net [49]	0.6840	0.8190	15.56
UNet++ [64]	0.6830	0.8110	18.27
BiO-Net [61]	0.7040	0.8240	15
Swin-Unet [5]	0.6377	0.7769	82.3
UCTransNet [56]	0.6668	0.7987	65.6
Proposed Mini-Net (lightweight)	**0.7056**	**0.8269**	**0.04**

5. CONCLUSION

In conclusion, Mini-Net offers a highly efficient and lightweight framework for real-time segmentation in medical imaging. Achieving state-of-the-art performance across diverse medical image datasets, it demonstrates both effectiveness and efficiency. With only 37,800 parameters, its compact architecture enables deployment on devices with limited memory and processing power. This makes Mini-Net well-suited for real-time medical applications in resource-constrained environments. Extensive experiments validate its strong generalizability across various medical imaging tasks. Its ability to maintain a balance between efficiency and performance enhances its practical applicability. The model's design ensures seamless integration into real-time medical imaging workflows. Mini-Net's adaptability supports its use in different clinical and diagnostic scenarios. Its low computational demands facilitate accessibility in settings with scarce resources. The framework's robustness underscores its potential in advancing healthcare technologies. By enabling real-time segmentation, Mini-Net enhances medical imaging efficiency. Thus, it serves as a transformative tool for improving diagnostic accuracy and healthcare outcomes.

REFERENCES

[1] Rakhshanda Imtiaz, Tariq M Khan, Syed Saud Naqvi, Muhammad Arsalan, and Syed Junaid Nawaz (2021). Screening of glaucoma disease from retinal vessel images using semantic segmentation. Computers & Electrical Engineering, 91:107036.

[2] Feilong Tang, Matt Trinh, Annita Duong, Angelica Ly, Fiona Stapleton, Zhe Chen, Zongyuan Ge, and Imran Razzak (2024). Discriminating retinal microvascular and neuronal differences related to migraines: Deep learning based cross-sectional study. arXiv preprint arXiv:2408.07293.

[3] Matt Trinh, Feilong Tang, Angelica Ly, Annita Duong, Fiona Stapleton, Zongyuan Ge, and Imran Razzak (2024). Sight for sore heads–using CNNs to diagnose migraines. Investigative Ophthalmology & Visual Science, 65(9): PB0010–PB0010.

[4] Tariq M Khan, Antonio Robles-Kelly, Syed S Naqvi, and Arsalan Muhammad (2021). Residual multiscale full convolutional network (RM-FCN) for high-resolution semantic segmentation of retinal vasculature. In Structural, Syntactic, and Statistical Pattern Recognition: Joint IAPR International Workshops, page 324–333.

[5] Tariq M Khan, Mohammad AU Khan, Naveed Ur Rehman, Khuram Naveed, Imran Uddin Afridi, Syed Saud Naqvi, and Imran Razzak (2022). Width-wise vessel bifurcation for improved retinal vessel segmentation. Biomedical Signal Processing and Control, 71:103169.

[6] Coen De Vente, Koenraad A Vermeer, Nicolas Jaccard, He Wang, Hongyi Sun, Firas Khader, Daniel Truhn, Temirgali Aimyshev, Yerkebulan Zhanibekuly, Tien-Dung Le, et al. (2023). AIROGS: Artificial intelligence for robust glaucoma screening challenge. IEEE Transactions on Medical Imaging, 43(1):542–557.

[7] Khuram Naveed, Faizan Abdullah, Hussain Ahmad Madni, Mohammad AU Khan, Tariq M Khan, and Syed Saud Naqvi (2021). Towards automated eye diagnosis: An improved retinal vessel segmentation framework using ensemble block matching 3D filter. Diagnostics, 11(1):114.

[8] S. K. Abrokwa, L. C. Ruby, C. C. Heuvelings, and S. Belard (2022). Task shifting for point-of-care ultrasound in primary healthcare in low-and middle-income countries—a systematic review. EClinicalMedicine, vol. 45.

[9] B. Dulmage, K. Tegtmeyer, M. Z. Zhang, M. Colavincenzo, and S. Xu (2021). A point-of-care, real-time artificial intelligence system to support clinician diagnosis of a wide range of skin diseases. Journal of Investigative Dermatology, vol. 141, no. 5, pp. 1230–1235.

[10] Tariq M Khan, Syed S Naqvi, and Erik Meijering (2022). Leveraging image complexity in macro-level neural network design for medical image segmentation. Scientific Reports, 12(1):22286.

[11] Shahzaib Iqbal, Saud Naqvi, Haroon Ahmed, Ahsan Saadat, and Tariq M Khan (2022). G-Net Light: A lightweight modified Google Net for retinal vessel segmentation. In Photonics, volume 9, pages 923–936. MDPI.

[12] Tariq M Khan, Muhammad Arsalan, Antonio Robles-Kelly, and Erik Meijering (2022). MKIS-Net: A light-weight multi-kernel network for medical image segmentation. In International Conference on Digital Image Computing: Techniques and Applications (DICTA), pages 1–8. 10.1109/DICTA56598.2022.10034573.

[13] Tariq M Khan, Muhammad Arsalan, Imran Razzak, and Erik Meijering (2023). Simple and robust depth-wise cascaded network for polyp segmentation. Engineering Applications of Artificial Intelligence, 121:106023.

[14] Tariq M Khan, Muhammad Arsalan, Shahzaib Iqbal, Imran Razzak, and Erik Meijering (2023). Feature Enhancer Segmentation Network (FES-Net) for vessel segmentation. arXiv preprint arXiv:2309.03535.

[15] Lang J, Liu Y (2023). LCCF-Net: Lightweight contextual and channel fusion network for medical image segmentation. Biomed Signal Process Control, 86:105134.

[16] Liu Y, Shen J, Yang L, et al. (2023). Wave-Net: A lightweight deep network for retinal vessel segmentation from fundus images. Comput Biol Med, 152:106341.

[17] J. M. J. Valanarasu and V. M. Patel (2022). UNeXt: MLP-based rapid medical image segmentation network. In Medical Image Computing and Computer-Assisted Intervention–MICCAI 2022: 25th International Conference, Singapore, September 18–22, 2022, Proceedings, Part V. Springer, pp. 23–33.

[18] J. Ruan, M. Xie, J. Gao, T. Liu, and Y. Fu (2023). EGE-UNet: An efficient group enhanced UNet for skin lesion segmentation. In International Conference on Medical Image Computing and Computer-Assisted Intervention. Springer, pp. 481–490.
[19] Y. Liu, H. Zhu, M. Liu, H. Yu, Z. Chen, and J. Gao (2024). Rolling-UNet: Revitalizing MLP's ability to efficiently extract long-distance dependencies for medical image segmentation. In Proceedings of the AAAI Conference on Artificial Intelligence, vol. 38, no. 4, pp. 3819–3827.
[20] C. Li, X. Liu, W. Li, C. Wang, H. Liu, and Y. Yuan (2024). U-KAN makes strong backbone for medical image segmentation and generation. arXiv preprint arXiv:2406.02918.
[21] Z. Liu, Y. Wang, S. Vaidya, F. Ruehle, J. Halverson, M. Soljačić, T. Y. Hou, and M. Tegmark (2024). KAN: Kolmogorov-Arnold networks. arXiv preprint arXiv:2404.19756.
[22] Mingxing Tan and Quoc Le (2019). EfficientNet: Rethinking model scaling for convolutional neural networks. In International Conference on Machine Learning, pages 6105–6114. PMLR.
[23] Yingping Li, Emilie Chouzenoux, Benoit Charmettant, Baya Benatsou, Jean-Philippe Lamarque, and Nathalie Lassau (2021). Lightweight U-Net for lesion segmentation in ultrasound images. In 2021 IEEE 18th International Symposium on Biomedical Imaging (ISBI), pages 611–615.
[24] Lang J, Liu Y (2023). LCCF-Net: Lightweight contextual and channel fusion network for medical image segmentation. Biomed Signal Process Control, 86:105134.
[25] Liu Y, Shen J, Yang L, et al. (2023). Wave-Net: A lightweight deep network for retinal vessel segmentation from fundus images. Comput Biol Med, 152:106341.
[26] Neeraj Kumar, Ruchika Verma, Deepak Anand, Yanning Zhou, Guanyu Cai, Xiaojie Liu, Yuqin Wang, and Amit Sethi (2020). A multiorgan nucleus segmentation challenge. *IEEE Transactions on Medical Imaging*, 39(5):1380–1391.

